Ion-Gated Electron Transfer in Self-Assembled Monolayer Films

Dean J. Campbell, Brian R. Herr, John C. Hulteen, Richard P. Van Duyne, and Chad A. Mirkin*

Contribution from the Department of Chemistry, Northwestern University, Evanston, Illinois 60208

Received June 3, 1996[⊗]

Abstract: The preparation and electrochemical characterization of self-assembled monolayers (SAMs) of azobenzenebutanethiols **1d** and ferrocenylazobenzenebutanethiols **2d** on Au are reported. Adsorption of these molecules onto Au surfaces has been verified by X-ray photoelectron spectroscopy and reflectance infrared spectroscopy. Optical ellipsometry, capacitance measurements, and cyclic voltammetry indicate that azobenzene-terminated adsorbate molecules form densely packed SAMs on Au(111). Reduction of the azobenzene group in **1d** or **2d** in an aprotic medium results in the formation of an azobenzene radical anion. However, SAMs of **1d** and **2d** exhibit almost no electrochemical accessibility for their azobenzene groups, even though a SAM of **2d** exhibits complete electrochemical accessibility for its outer layer of ferrocenyl groups. The azobenzene electrochemical inaccessibility is due to the densely packed structures of these SAMs and their ability to prohibit the incorporation of charge-compensating cations upon their reduction. Addition of free volume to a film of **2d** by coadsorption with ethanethiol or more efficient use of the existing free volume in a full monolayer by using smaller charge-compensating cations such as H^+ or Li^+ results in greater azobenzene accessibility. Therefore, electron transfer processes between the electrode surface and the redox-active azobenzene centers within the film can be gated by controlling charge-compensating cation size and concentration and/or film structure. This gating behavior constitutes a supramolecular response in SAMs as it is a collective property of the film and not a property of the molecules that comprise the film. Reduction of the azobenzene in the SAM in the presence of H^+ results in hydrazobenzene formation, which has been verified by Raman spectroelectrochemistry. The potential for the latter reduction is dependent upon pH. A three-case model has been proposed to describe the ion-gating behavior of a SAM of **2d**.

Introduction

"Self-assembled" monolayers (SAMs) are films formed from the chemisorption of a single layer of adsorbate molecules from solution or the gas phase onto a surface of interest, and they have been extensively studied because of their enormous utility in tailoring surface properties. Through choice of adsorbate molecule, the reactivity, wetting, adhesive, electrical, and structural properties of a surface can be exquisitely controlled.[1] SAMs have been used to develop novel surface-patterning methodologies,[2] fabricate new types of chemically sensitive devices,[3] study interfacial electron transfer processes,[1,4] and prepare a variety of unusual and potentially useful electronic, photonic, and redox-active materials.[3−6] In addition, SAMs have been used as passivating layers to stabilize numerous materials including the very reactive class of cuprate-based high-temperature superconductors.[7]

A key set of issues regarding SAMs pertains to the chemical and physical consequences of adsorbate surface attachment, dense packing, and self-organization. In the molecular biology literature "self-assembly" not only implies the formation of an ordered, definable structural unit but also implies an element of supramolecular function.[8−10] With proteins and lipid bilayers

* To whom correspondence should be addressed.

[⊗] Abstract published in *Advance ACS Abstracts,* October 1, 1996.

(1) For reviews on monolayer films, see: (a) Bain, C. D.; Whitesides, G. M. *Angew. Chem., Int. Ed. Engl.* **1989**, *28*, 506. (b) Dubois, L. H.; Nuzzo, R. G. *Annu. Rev. Phys. Chem.* **1992**, *43*, 437. For additional manuscripts describing electron transfer phenomena in monolayer films, see: (c) Finklea, H. O.; Avery, S.; Lynch, M.; Furtsch, T. *Langmuir* **1987**, *3*, 409. (d) Finklea, H. O.; Hanshew, D. D. *J. Am. Chem. Soc.* **1992**, *114*, 3173. (e) Chidsey, C. E. D. *Science* **1991**, *251*, 919. (f) Tender, L.; Carter, M. T.; Murray, R. W. *Anal. Chem.* **1994**, *66*, 3173. (g) Weber, K.; Creager, S. E. *Anal. Chem.* **1994**, *66*, 3164. (h) Li, T. T. T.; Weaver, M. J. *J. Am. Chem. Soc.* **1984**, *106*, 6107. (i) Creager, S. E.; Weber, K. *Langmuir* **1993**, *9*, 844. (j) Lenhard, J. R.; Murray, R. W. *J. Am. Chem. Soc.* **1978**, *100*, 7870. (k) Bumm, L. A.; Arnold, J. J.; Cygan, M. T.; Dunbar, T. D.; Burgin, T. P.; Jones, L., II; Allara, D. L.; Tour, J. M.; Weiss, P. S. *Science* **1996**, *271*, 1705. (l) Richardson, J. N.; Peck, S. R.; Curtin, L. S.; Tender, L. M.; Terrill, R. H.; Carter, M. T.; Murray, R. W.; Rowe, G. K.; Creager, S. E. *J. Phys. Chem.* **1995**, *99*, 766.

(2) (a) Wollman, E. W.; Kang, D.; Frisbie, C. D.; Lorkovic, I. M.; Wrighton, M. S. *J. Am. Chem. Soc.* **1994**, *116*, 4395. (b) Wollman, E. W.; Frisbie, C. D; Wrighton, M. S. *Langmuir* **1993**, *9*, 1517. (c) Tarlov, M. J.; Burgess, D. R. F., Jr.; Gillen, G. *J. Am. Chem. Soc.* **1993**, *115*, 5305.

(3) (a) Mirkin, C. A.; Ratner, M. A. *Annu. Rev. Phys. Chem.* **1992**, *43*, 719. (b) Mirkin, C. A.; Valentine, J. R.; Ofer, D.; Hickman, J. J.; Wrighton, M. S. In *Biosensors and Chemical Sensors: Optimizing Performance Through Polymeric Materials*; Edelman, P. G., Wang, J., Eds.; ACS Symposium Series 487; American Chemical Society: Washington, DC, 1992; Chapter 17. (c) Hickman, J. J.; Ofer, D.; Laibinis, P. E.; Whitesides, G. M.; Wrighton, M. S. *Science* **1991**, *252*, 688.

(4) (a) Herr, B. R.; Mirkin, C. A. *J. Am. Chem. Soc.* **1994**, *116*, 1157. (b) Herr, B. R.; Mirkin, C. A. *Proc. Am. Chem. Soc. Div. Polym. Mater. Sci. Eng.* **1994**, *71*, 775. (c) Uosaki, K.; Sato, Y.; Kita, H. *Electrochim. Acta* **1991**, *36*, 1799. (d) Sato, Y.; Itoigawa, H.; Uosaki, K. *Bull. Chem. Soc. Jpn.* **1993**, *66*, 1032. (e) De Long, H. C.; Buttry, D. A. *Langmuir* **1992**, *8*, 2491. (f) De Long, H. C.; Buttry, D. A. *Langmuir* **1990**, *6*, 1319.

(5) Li, D.; Ratner, M. A.; Marks, T. J.; Zhang, C. H.; Yang, J.; Wong, G. K *J. Am. Chem. Soc.* **1990**, *112*, 7389.

(6) (a) Kawanishi, Y.; Tamaki, T.; Sakuragi, M.; Seki, T.; Suzuki, Y.; Ichimura, K. *Langmuir* **1992**, *8*, 2601. (b) Ichimura, K.; Suzuki, Y.; Seki, T.; Hosoki, A.; Aoki, K. *Langmuir* **1988**, *4*, 1214.

(7) (a) Chen, K.; Mirkin, C. A.; Lo, R.-K.; Zhou, J.-P.; McDevitt, J. T. *J. Am. Chem. Soc.* **1995**, *117*, 6374. (b) McDevitt, J. T.; Mirkin, C. A.; Lo, R.-K.; Chen, K.; Zhou, J.-P.; Xu, F.; Haupt, S. G., Zhao, J.; Jurbegs, D. C. *Chem. Mater.* **1996**, *8*, 811. (c) Chen, K.; Xu, F.; Mirkin, C. A.; Lo, R.-K.; Nanjundaswamy, K. S.; Zhou, J.-P.; McDevitt, J. T. *Langmuir* **1996**, *12*, 2622.

(8) Johnson, L. J. *Biology,* 2nd ed.; Wm. C. Brown: Dubuque, IA, 1987.

(9) (a) Fox, S. W.; Dose, K. *Molecular Evolution and the Origin of Life,* revised ed.; Marcel Dekker: New York, 1977. (b) Schmitt, F. O. *Proc. Am. Philos. Soc.* **1956**, 100, 476.

S0002-7863(96)01873-2 CCC: $12.00

this is easily understood through the complex functions these structures perform in spite of the relatively simple molecules used to construct them. Interestingly, by analogy there are very few recognized examples of supramolecular behavior in self-assembled monolayers. In part, this could be due to the relatively simple molecules used thus far to construct such films. A key question is: can an organized monolayer have a set of properties that are distinct from the adsorbate molecules that comprise it, and if so, can these properties be correlated with film structure? One of our long-standing goals has been to develop new adsorbate molecules that both are conducive to forming highly ordered monolayer films and exhibit interesting chemical reactivity and electroactivity. These molecules allow one to probe the chemical and physical consequences of organizing adsorbate molecules from solution onto surfaces of interest. In our group, two properties of interest include concerted reactivity utilizing the organized array that a SAM can provide and electron transfer within and across the film.

The experiments reported herein elucidate the relationship between monolayer structure and electrochemical response for SAMs formed from surface-confinable azobenzenes **1** and ferrocenylazobenzenes **2**. The azobenzene group is redox-active

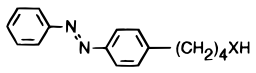

1a, X = O
1d, X = S

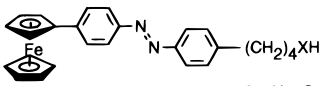

2a, X = O
2d, X = S

and chemically reactive and has vibrational transitions with large Raman and IR cross-sections,[11] making it an attractive candidate for a variety of chemical and spectroscopic studies. Furthermore, the azobenzene group has been shown to be conducive to forming highly ordered SAM structures.[12,13] Finally, the ferrocenyl group is redox-active and has been extensively used by our group[4a,b,7b] and others[1,4c−f] to study the electrochemical properties of SAMs.

In this study, we focus on the relationship between monolayer film structure and the electron transfer processes between the Au electrode surface and the redox-active centers within films formed from **1d** or **2d**. Herein, we show that, in the case of films formed from **2d**, film structure can be used to control ion transport from solution to the azobenzene redox centers within the monolayer and, in doing so, can effectively turn on or off electron transfer processes between the electrode surface and the azobenzene groups within the film. Furthermore, we show that electron transfer processes between the Au and the azobenzene redox centers within these novel films may be "gated" by controlling the size and concentration of the charge-compensating cations or by manipulating the structure of the film. Significantly, this is a clear example of supramolecular function in the context of a SAM, and interestingly, there is a correlation between the type of ion-gating reported herein and that which occurs in macromolecular self-assembled biological systems.[15] Other types of ion-gating have also been observed for polymer films[16,17] and even solid-state materials.[18] A preliminary account of this work was previously communicated.[4a]

Experimental Section

SAM Preparation. In a typical experiment, freshly prepared Au substrates were immersed for 48 h at 22 °C in a 1 mM cyclohexane solution of the adsorbate molecule of interest. The wafers were removed from solution, vigorously rinsed with cyclohexane and dichloromethane, and blown dry with prepurified grade N_2 prior to use. Au substrates were prepared according to literature methods.[12,14]

X-ray Photoelectron Spectroscopy. Measurements were made by a VG Scientific ESCALAB MKII X-ray photoelectron spectrometer in a vacuum chamber at a pressure of 10^{-9} Torr. The angle of incidence of the Al source was ~45° with respect to the sample surface normal, and photoelectrons were collected at ~20° to the surface normal.

Ellipsometry. A Sopra MOSS ES 4 G spectroscopic ellipsometer was used to determine the film thickness for SAMs of **2d** on Au. Before and after monolayer adsorption, the ellipsometric parameters tan ψ and cos Δ were acquired from 600 to 820 nm at 10 nm intervals at an angle of 70° with respect to the surface normal. Each data point represents an average of 3 measurements/λ. In this range, the molecules that comprise the monolayer are transparent; therefore, in fitting the experimental data, the imaginary portion of the refractive index was disregarded ($k = 0$). The real refractive index (n) was assumed to be 1.60, in accordance with the known values for ethylferrocene (1.60),[19] azobenzene (1.63),[20] and butanethiol (1.44).[20] The data were modeled in the multilayer regression mode with the number of layers set equal to 1 and referenced to an octadecanethiol SAM, which on the basis of literature precedent was assumed to be 23.8 Å thick.[21] The data were modeled in the multilayer regression mode with the number of layers set equal to 1. The thicknesses reported for the monolayers represent an average of 6−8 measurements with an error of 2 Å.

Raman Spectroscopy. A Spectra Physics Model 124B HeNe laser was used for $\lambda_{ex} = 632.8$ nm, and $\lambda_{ex} = 752.0$ nm was obtained from a Spectra Physics Tsunami mode-locked Ti/Al_2O_3 laser pumped by a Coherent INNOVA 400 Ar^+ laser. The Ar^+ also provided $\lambda_{ex} = 501.7$ and 514.8 nm. Surface-enhanced Raman spectroscopy (SERS) measurements at $\lambda_{ex} = 632.8$ nm were obtained on an ACTON VM-505 single grating monochromator equipped with a Photometrics PM-512 CCD detector. Holographic edge filters (Physical Optics Co.) were used for exclusion of λ_{ex}. For spectra recorded at $\lambda_{ex} = 501.7$, 514.8, and 752.0 nm, a SPEX Model 1877 Triplemate triple grating monochromator equipped with 600 grooves/nm gratings blazed at 750 nm in the filter stage, 1200 grooves/nm in the spectrograph stage, and a SPEX Spectrum One CCD detector were used. For $\lambda_{ex} = 752.0$ nm,

(10) (a) Mucic, R. C.; Storhoff, J. S.; Letsinger, R. L.; Mirkin, C. A., *Nature* **1996**, *382*, 607. (b) Gottarelli, G.; Masiero, S.; Spada, G. P. *J. Chem. Soc., Chem. Commun.* **1995**, 2555.

(11) (a) Womack, J. D.; Vickers, T. J.; Mann, C. K. *Appl. Spectrosc.* **1987**, *41*, 117. (b) Klima, M. I.; Kotov, A. V.; Gribov, L. A. *Zh. Strukt. Khim.* **1972**, *13*, 987. (c) Kellerer, B.; Hacker, H. H.; Brandmüller, J. *Indian J. Pure Appl. Phys.* **1971**, *9*, 903. (d) Trotter, P. J. *Appl. Spectrosc.* **1977**, *31*, 30. (e) Armstrong, D. R.; Clarkson, J.; Smith, W. E. *J. Phys. Chem.* **1995**, *99*, 17825.

(12) Caldwell, W. B.; Campbell, D. J.; Chen, K.; Herr, B. R.; Mirkin, C. A.; Malik, A.; Durbin, M. K.; Dutta, P.; Huang, K. G. *J. Am. Chem. Soc.* **1995**, 117, 6071.

(13) (a) Jaschke, M.; Schönherr, H.; Wolf, H.; Butt, H.-J.; Bamberg, E.; Besocke, M. K.; Ringsdorf, H. *J. Phys. Chem.* **1996**, *100*, 2290. (b) Takami, T.; Delamarche, E.; Michel, B.; Gerber, Ch.; Wolf, H.; Ringsdorf, H. *Langmuir* **1995**, *11*, 3876. (c) Wolf, H.; Ringsdorf, H.; Delamarche, E.; Takami, T.; Kang, H.; Michel, B.; Gerber, Ch.; Jaschke, M.; Butt, H.-J.; Bamberg, E. *J. Phys. Chem.* **1995**, *99*, 7102.

(14) (a) Caldwell, W. B.; Chen, K.; Herr, B. R.; Mirkin, C. A.; Hulteen, J. C.; Van Duyne, R. P. *Langmuir* **1994**, *10*, 4109. (b) Chidsey, C. E. D.; Loiacono, D. N.; Sleator, T.; Nakahara, S. *Surf. Sci.* **1988**, *200*, 45. (c) Goss, C. A.; Brumfield, J. C.; Irene, E. A.; Murray, R. W. *Langmuir* **1993**, *9*, 2986.

(15) (a) Friedman, M. H. *Principles and Models of Biological Transport;* Springer-Verlag: Berlin, Germany, 1986; pp 50−59. (b) Stryer, L. *Biochemistry*, 3rd ed.; W. H. Freeman and Co.: New York, 1988; pp 969−971. (c) Nakashima, N.; Taguchi, T.; Takada, Y.; Fujio, K.; Kunitake, M.; Manabe, O. *J. Chem. Soc., Chem. Commun.* **1991**, 232. (d) Alberts, B.; Bray, D.; Lewis, J.; Raff, M.; Roberts, K.; Watson, J. D. *Molecular Biology of the Cell*, 3rd ed.; Garland Publishing: New York, 1994; pp 523−525.

(16) (a) Pressprich, K. A.; Maybury, S. G.; Thomas, R. E.; Linton, R. W.; Irene, E. A.; Murray, R. W. *J. Phys. Chem.* **1989**, *93*, 5568. (b) McCarley, R. L.; Irene, E. A.; Murray, R. W. *J. Phys. Chem.* **1991**, *95*, 2492.

(17) Huang, J.; Wrighton, M. S. *Anal. Chem.* **1993**, *65*, 2740.

(18) Chun, J. K. M.; Bocarsly, A. B.; Cottrell, T. R.; Benzinger, J. B.; Yee, J. C. *J. Am. Chem. Soc.* **1993**, *115*, 3024.

(19) Rosenblum, M. *Chemistry of the Iron Group Metallocenes: Ferrocene, Ruthocene, Osmocene*; John Wiley & Sons: New York, 1965; Part 1, p 153.

(20) Chemical Rubber Co. *CRC Handbook of Chemistry and Physics*, 70th ed.; CRC Press: Boca Raton, FL, 1989.

(21) Porter, M. D.; Bright, T. B.; Allara, D. L.; Chidsey, C. E. D. *J. Am. Chem. Soc.* **1987**, *109*, 3559.

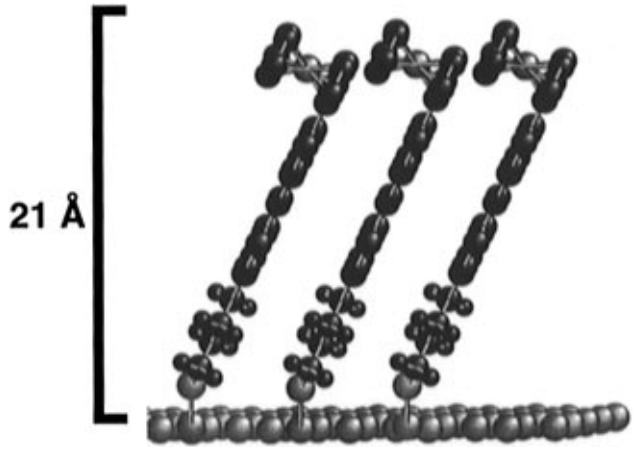

Figure 1. Computer-generated (SYBYL) drawing of **2d** on Au(111).

a band-pass filter (Oriel Corp., Stratford, CT) centered at 750 nm with a 10 nm fwhm was utilized for removing energy at exogenous wavelengths. The angle of incidence of the laser excitation source was ~45° with respect to the surface normal, and Raman scattered light was collected along the surface normal.

The spectroelectrochemical cell was constructed from Teflon, Kel-F, and stainless steel materials. The cell was air-free, greaseless, and epoxy-free, and its working volume was ~1 mL. The SERS-active working electrode consisted of a Au film grown by thermal vapor deposition (r_d = 0.03 nm/s, d_m = 100 nm) on a Ag rod (99.95%, 5.0 mm diameter, D. F. Goldsmith) that was sheathed in Teflon. For additional surface signal enhancement, a Au film over a nanosphere (AuFon) surface was prepared by depositing carboxypolystyrene nanospheres (495 nm diameter, Interfacial Dynamics Corp.) on a Ag rod followed by Au deposition.[22]

Infrared External Reflection Spectroscopy. Infrared external reflection spectroscopy was performed using a Nicolet 730 Fourier transform infrared spectrometer with a Spectra-Tech FT-85 grazing angle accessory. The refractive geometry of the accessory allowed only p-polarized light to impinge upon the sample with an 85° incident angle. Spectra were taken using 512 scans at 2 cm^{-1} resolution. Large (2.5 cm × 8 cm) Au(111)/mica substrates were modified with thiols for this spectral study.

Results and Discussion

SAMs of 1d and 2d on Au(111)/Mica: Preparation and Characterization by X-ray Photoelectron Spectroscopy, Ellipsometry, and Differential Capacitance. SAMs of **1d** and **2d** on Au(111)/mica were characterized by X-ray photoelectron spectroscopy (XPS), ellipsometry, and differential capacitance measurements. A SAM of a longer chain version of **1d** has been structurally characterized in air by synchrotron in-plane X-ray diffraction and atomic force microscopy.[12] The general chemical and physical properties of **1d** seem to mirror those of its longer chain counterpart (see Electrochemistry section). Therefore, most of our surface characterization efforts have focused on SAMs of **2d**. Analysis of SAMs of **2d** by XPS gives characteristic elemental signatures: S (2p), 163 eV; C (1s), 285 eV; N (1s), 401 eV; Fe ($2p_{3/2}$), 720 eV. In addition, the ellipsometrically determined thicknesses for a SAM of **2d** on Au(111) is 21 ± 2 Å. Note that the ellipsometrically determined thickness of the film is approximately equal to the length of the adsorbate molecule, assuming an all-*anti* conformation for the alkane chain, Figure 1. This is consistent with the assignment of an upright orientation for the adsorbate molecules that comprise a SAM of **2d**. It should be noted that ellipsometrically determined film thicknesses are model dependent. However, varying the refractive index by 0.1 changed the calculated film thickness by only 2 Å, and therefore, errors in assumed refractive indices would not alter the conclusions that are drawn from these data.

SAM interactions with the electrochemical double layer can be modeled as a parallel-plate capacitor according to the Helmholtz model and therefore are represented by the equation $C_d = \epsilon\epsilon_o/d$, where C_d is the differential capacitance, ϵ is the dielectric constant of the medium, ϵ_o is the permittivity of free space, and d is the interplate spacing or the distance between the electrode surface and the charge-compensating ions. For the experiments described herein, d is the ellipsometrically determined film thickness. This model has been used previously to examine the charging current of Au electrodes modified with SAMs of alkanethiols and to make arguments regarding the ability of the SAM to act as a barrier layer between the electrode and ions in solution.[21] By contrast the behavior of bare Au electrodes cannot be described well by the Helmholtz model because the bare Au capacitances are dependent upon electrode potential and the nature of the electrolyte media.[23] For perfectly flat electrodes the theoretical capacitance values for the SAMs are 0.89 μF/cm^2 for octadecanethiol, 1.4 μF/cm^2 for **1d**, and 1.1 μF/cm^2 for **2d**. This yields capacitance ratios of 1.6 for **1d** to octadecanethiol and 1.2 for **2d** to octadecanethiol. The advantage of examining capacitance ratios instead of the capacitance values themselves is that the capacitance measurements are susceptible to nonidealities such as surface roughness, which increases surface area.[21] Using capacitance *ratios* minimizes these problems. The measured capacitance ratios are 2.3 for **1d** to octadecanethiol and 1.7 for **2d** to octadecanethiol. The similarity between theoretical and experimental ratios indicates that SAMs of **1d** and **2d** are densely packed like those of octadecanethiol. The fact that the experimental ratios are slightly higher than the theoretical ratios may be due to the dielectric constant of the real films being slightly higher than theory predicts. If a polar solvent such as water partitions into the azobenzene SAMs better than the octadecanethiol SAMs, the dielectric constant of the azobenzene films will be higher.[21]

Electrochemistry of 1a and 2a. Compounds **1a** and **2a** exhibit typical azobenzene electrochemical behavior in both protic and aprotic solvents.[24] For example, in THF **2a** (0.8 mM) undergoes a reversible one-electron reduction to form a radical anion, $E_{1/2}$ = −1.91 V vs Fc/Fc^+, eq 1 and Figure 2A (—). The

$$\mathrm{R{-}Ar{-}N{=}N{-}Ar{-}Fc} \underset{-e^-}{\overset{+e^-}{\rightleftharpoons}} [\mathrm{R{-}Ar{-}N{=}N{-}Ar{-}Fc}]^{\bullet -} \underset{-e^-,\,H^+}{\overset{+e^-,\,H^+}{\rightleftharpoons}} [\mathrm{R{-}Ar{-}NH{-}N{-}Ar{-}Fc}]^- \quad (1)$$

radical anion will undergo a further one-electron, one-proton reduction, E_{pc} = −2.44 V vs Fc/Fc^+, to form a monoprotonated dianion, eq 1. Compound **1a** undergoes comparable processes. In addition to azobenzene-based electrochemistry, **2a** undergoes a ferrocenyl-centered one-electron oxidation to form a ferrocenium species, $E_{1/2}$ = 0.030 V vs Fc/Fc^+, eq 2. In protic media

(22) For similar work with silver films, see: (a) Yang, W.; Hulteen, J.; Schatz, G. C.; Van Duyne, R. P. *J. Chem. Phys.* **1996**, *104*, 4313. (b) Van Duyne, R. P.; Hulteen, J. C.; Treichel, D. A. *J. Chem. Phys.* **1993**, *99*, 2101.

(23) (a) Schmid, G. M.; Curley-Fiorno, M. E. *Encyclopedia of Electrochemistry of the Elements;* Bard, A. J., Ed.; Marcel Dekker, Inc.: New York, 1975; Vol. IV, pp 118−124. (b) Bard, A. J.; Faulkner, L. R. *Electrochemical Methods: Fundamentals and Applications;* John Wiley & Sons: New York, 1980; pp 500−515.

(24) (a) Sadler, J. L.; Bard, A. J. *J. Am. Chem. Soc.* **1968**, *90*, 1979. (b) Boto, K. G.; Thomas, F. G. *Aust. J. Chem.* **1973**, *26*, 1251. (c) Yu, H.-Z.; Wang, Y.-Q.; Cheng, J.-Z.; Zhao, J.-W.; Cai, S.-M.; Inokuchi, H.; Fujishima, A.; Liu, Z.-F. *Langmuir* **1996**, *12*, 2843.

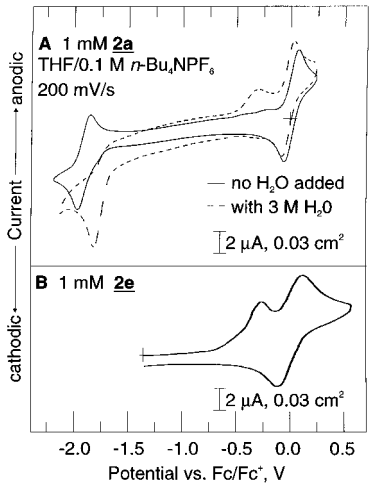

Figure 2. (A) Cyclic voltammetry for **2a** at a Au disk electrode: (—) in aprotic THF/0.1 M n-Bu_4NPF_6 electrolyte and (- - -) in THF/0.1 M n-Bu_4NPF_6 electrolyte containing 3 M H_2O. (B) Cyclic voltammetry for **2e** at a Au disk electrode in aprotic THF/0.1 M n-Bu_4NPF_6 electrolyte.

$$R{-}Ar{-}N{=}N{-}Ar{-}Fc \underset{+e^-}{\overset{-e^-}{\rightleftharpoons}} [R{-}Ar{-}N{=}N{-}Ar{-}Fc]^+ \quad (2)$$

(THF with 3 M H_2O) **2a** undergoes a two-electron, two-proton reduction, $E_{pc} = -1.82$ V vs Fc/Fc^+, to form a ferrocenylhydrazobenzene species that is reoxidized in another two-electron, two-proton process, $E_{pa} = -0.32$ V vs Fc/Fc^+, to re-form the parent ferrocenylazobenzene, eq 3 and Figure 2A (- - -). Sig-

$$R{-}Ar{-}N{=}N{-}Ar{-}Fc \underset{-2e^-,\,2H^+}{\overset{+2e^-,\,2H^+}{\rightleftharpoons}} R{-}Ar{-}NH{-}NH{-}Ar{-}Fc \quad (3)$$

nificantly, this latter assignment has been confirmed by synthesizing, isolating, and electrochemically characterizing an authentic sample of the ferrocenylhydrazobenzene compound **2e**, Figure 2B. Compound **2e** is oxidized electrochemically in THF/0.1 M n-Bu_4NPF_6 to form **2d**, $E_{pa} = -0.25$ V vs Fc/Fc^+. The potentials at which these processes occur are helpful, but not absolutely diagnostic, in characterizing the products formed upon oxidation and reduction of monolayer films of azobenzene compounds **1d** and **2d**. Surface-enhanced Raman spectroelectrochemistry also has been used to elucidate the products formed from reduction of the monolayers *(vide infra)*.

Electrochemistry for Monolayer Films of 1d and 2d. Cyclic voltammetry of a monolayer of **1d** on Au(111)/mica in aprotic solvents, Figure 3A, shows very little electroactivity associated with the azobenzene moiety in a potential window that extends several hundred millivolts past where solution **1a** is reduced, Figure 2A. In THF/0.1 M n-Bu_4NPF_6, the monolayer of **1d** exhibits a small reversible redox wave associated with radical anion formation at -1.96 V vs Fc/Fc^+. Integration of the current associated with azobenzene reduction yields an *electrochemical accessibility* of 5.8×10^{-11} mol/cm^2, which is approximately 6% of a full monolayer. This lack of electroactivity for the **1d** SAM is consistent with what has been reported for a longer chain analogue of **1d**, p-$HS(CH_2)_{11}$-$OC_6H_4N{=}NC_6H_5$.[12] In addition, the monolayer of **1d** is an excellent barrier layer that significantly inhibits electron transfer between the Au surface and dissolved ferricyanide anions, Figure 4A. Figure 4B shows that the electrode becomes accessible to ferricyanide after holding at potentials sufficient to desorb the monolayer. We and others have noted this reductive desorption

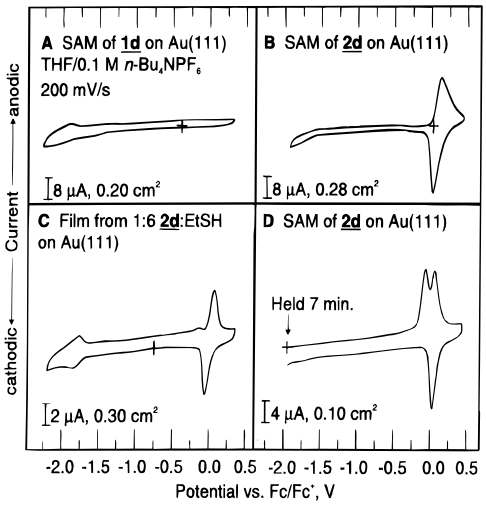

Figure 3. (A) Cyclic voltammetry for a SAM of **1d** on Au(111)/mica. (B) Cyclic voltammetry for a SAM of **2d** on Au(111)/mica. (C) Cyclic voltammetry for a monolayer film made from a 1:6 solution ratio of **2d** to ethanethiol on Au(111)/mica. (D) Cyclic voltammetry for a SAM of **2d** on Au(111)/mica after holding for 7 min at -1.9 V vs Fc/Fc^+. All electrochemical measurements were made in aprotic THF/0.1 M n-Bu_4NPF_6 electrolyte.

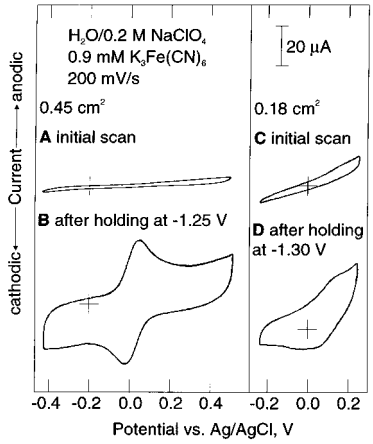

Figure 4. Cyclic voltammetry for 0.9 mM $K_3Fe(CN)_6$ in H_2O/0.2 M $NaClO_4$ (A) at a SAM of **1d** on Au(111)/mica, (B) at the same SAM after holding at -1.25 V, (C) at a SAM of **2d** on Au(111)/mica, and (D) at the same SAM after holding at -1.30 V.

process for a wide range of thiol adsorbate molecules.[12,25−27] By contrast, a monolayer of **2d** shows *no* detectable electroactivity for the azobenzene groups that comprise the film, but exhibits a response typical of surface-confined ferrocenyl adsorbate molecules, Figure 3B. If one assumes that the ferrocenyl moieties are completely electrochemically accessible in this film, integration of the current associated with ferrocenyl oxidation/reduction gives a surface coverage of 5.1×10^{-10} mol/cm^2.[4a,b] If **2d** is standing upright, the ferrocenyl moiety dictates its molecular footprint and, therefore, the upper limit for adsorbate surface coverage. If the molecule is lying on the surface, the ferrocenyl moiety and the azobenzenealkanethiol tether will increase its effective footprint and substantially decrease the expected surface coverage. Taking into account the most efficient way **2d** can pack on the Au(111) and a Au roughness factor of 1.3,[14a] the maximum surface coverage for **2d** is 5.8×10^{-10} mol/cm^2. The monolayer of **2d** also is an

(25) Schneider, T. W.; Buttry, D. A. *J. Am. Chem. Soc.* **1993**, *115*, 12391.
(26) Widrig, C. A.; Chung, C.; Porter, M. D. *J. Electroanal. Chem.* **1991**, *310*, 335.
(27) Weishaar, D. E.; Lamp, B. D.; Porter, M. D. *J. Am. Chem. Soc.* **1992**, *114*, 5860.

excellent barrier layer that significantly inhibits electron transfer between the Au surface and dissolved ferricyanide anions, Figure 4C. Like the electrode modified with **1d**, this electrode becomes accessible to ferricyanide after holding at potentials sufficient to desorb the monolayer, Figure 4D. Therefore, the electrochemically assayed surface coverage, ion penetration experiments, and ellipsometric data for a monolayer of **2d** strongly suggest that the adsorbate molecules are densely packed and standing upright, and the ferrocenyl groups are completely electrochemically accessible.

The broadened waves associated with ferrocenyl oxidation/reduction in films of **2d** also are consistent with densely packed SAMs. At a sweep rate of 200 mV/s, the wave associated with ferrocenyl oxidation in a SAM of **2d** on Au has a full width at half-maximum (fwhm) of 214 mV, and the wave associated with reduction of surface-confined ferrocenium has a fwhm of 118 mV. Decreasing the sweep rate reduces the peak-to-peak separation to nearly zero, but the waves still retain their assymetrical shapes and exhibit fwhms greater than 90 mV. This wave broadening, which has been modeled theoretically and measured experimentally for other redox-active adsorbates, has been attributed to adsorbate−adsorbate repulsive interactions, potential drop effects, and heterogeneities in the monolayer film.[28−30] Significantly, at lower surface coverages of **2d** (at 50% monolayer coverage) both ferrocenyl waves exhibit more ideal behavior with fwhms of 100 mV at 200 mV/s, Figure 3C, which also match theoretical predictions and experimental observations on comparable systems.[28−30]

If one assumes an upright orientation of **2d** in the monolayer, then the electrochemical response for the film is quite peculiar. Essentially, the redox-active ferrocenylazobenzenebutanethiol molecules have formed a redox bilayer where the layer of redox groups farthest from the electrode surface (the ferrocenyl groups) are electrochemically accessible, and those closest to the surface (the azobenzene groups) are *completely* inaccessible. This result is somewhat counterintuitive if a comparison is made between traditional polymeric redox bilayers and the redox bilayer formed from **2d**. In the former structure type, the layer closest to the electrode surface mediates electron transfer between the electrode and the outer layer.[3a] In the monolayer/redox bilayer formed from adsorption of **2d** on Au(111), the inner azobenzene layer does not appear to significantly affect electron transfer processes between the ferrocenyl groups and the Au surface.

Experiments Designed To Determine the Role of Ion Transport in SAMs of 2d. In view of the densely packed structure of **2d** on Au, we propose that the origin of the electrochemical inaccessibility of the azobenzene groups is due in part to film exclusion of charge-compensating cations from its interior azobenzene groups. To test this assumption, we performed a series of experiments designed to probe the effects of inhibited ion transport in such film structures and their relationship with electrode−adsorbate electron transfer processes. For example, when a Au electrode modified with **2d** is held for 7 min at a negative potential sufficient to reduce the azobenzene (in solution), and then brought to a positive potential sufficient to reoxidize the SAM, an oxidative wave associated with the conversion of the reduced hydrazobenzene species to the parent azobenzene is observed, Figure 3D. The oxidation wave, $E_{pa} = -0.070$ V vs Fc/Fc^+, is consistent with reoxidation of a ferrocenylhydrazobenzene species rather than a radical anion or monoprotonated dianion; Raman spectroscopy studies confirm this assignment (*vide infra*). Apparently reduction of the azobenzene groups does not take place until a H^+ source can work its way into the film. The H^+ source is most likely trace H_2O from the glassware or electrolyte; it is not coming from the solvent *(vide infra)*. In this experiment, approximately 40% (1.8×10^{-10} mol/cm^2) of the azobenzenes within the SAM are being accessed electrochemically as determined by comparing the currents associated with hydrazobenzene and ferrocenium redox waves. Note that this experiment is not a measure of the maximum number of azobenzenes that can be reduced within the SAM since approximately 10% of the monolayer is removed in the experiment. This is evidenced by a decrease in the Faradaic current associated with the ferrocene/ferrocenium redox couple after the holding experiment has taken place; the ferrocene/ferrocenium redox couple therefore serves as an internal reference in the system.

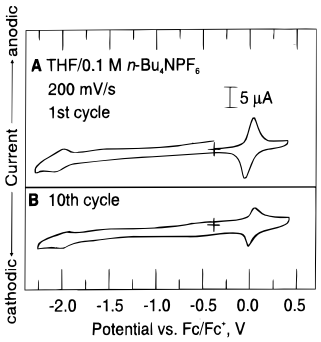

Figure 5. Cyclic voltammetry for a monolayer film prepared from a 1:6 solution ratio of **2d** to ethanethiol on Au(111)/mica: (A) initial cycle and (B) 10th cycle to −2.3 V vs Fc/Fc^+. All electrochemical measurements were made in aprotic THF/0.1 M n-Bu_4NPF_6 electrolyte.

Monolayers Formed from the Coadsorption of 2d and 1d with Ethanethiol: **Probing the Effects of Increased Free Volume on the Electron Transfer Properties of Surface-Confined Adsorbates.** Wafers soaked for 48 h in a 1:6 **2d**/ethanethiol solution in cyclohexane exhibited substantial azobenzene accessibility, Figure 3C. The electrochemical accessibility of the ferrocenyl group in **2d** is used to determine the surface ratio of **2d** to ethanethiol. Integration of the current associated with oxidation of the ferrocenyl groups in the coadsorbed monolayer yielded a surface coverage of 3×10^{-10} mol/cm^2. This is approximately 52% of a full monolayer and suggests substantial incorporation of ethanethiol into the film. Taking into account literature values for a full monolayer of an alkanethiol on Au(111) and an estimated surface roughness factor of 1.3,[14a] we estimate the surface ratio of **2d** to ethanethiol to be 3:7. It is not so surprising that the surface ratio of adsorbate molecules does not reflect their solution ratio; others have found similar differences in the solution and surface ratios of adsorbate molecules for alcohol and methyl-terminated alkanethiol systems[31] and for ferrocenyl- and methyl-terminated alkanethiol systems.[29]

Interestingly, even upon coadsorption of **2d** with ethanethiol, the electrochemical *accessibility* of the azobenzene groups is still substantially low. For example, Figure 5A shows the voltammogram of a coadsorbed monolayer (solution ratio 1:6, soaking time 20 min). The initial electrochemical accessibilities of the ferrocenyl and azobenzene groups are 2.5×10^{-10} and

(28) (a) Murray, R. W. In *Electroanalytical Chemistry: A Series of Advances;* Bard, A. J., Ed.; Marcel Dekker: New York, 1984; Vol. 13, pp 191−368. (b) Collard, D. M.; Fox, M. A. *Langmuir* **1991**, *7*, 1192. (c) Brown, A. P.; Anson, F. C. *Anal. Chem.* **1977**, *49*, 1589.

(29) Chidsey, C. E. D.; Bertozzi, C. R.; Putvinski, T. M.; Mujsce, A. M. *J. Am. Chem. Soc.* **1990**, *112*, 4301.

(30) (a) Smith, C. P.; White, H. S. *Anal. Chem.* **1992**, *64*, 2398. (b) Smith, C. P.; White, H. S. *Proceedings of the Symposium on Microscopic Models of Electrode Electrolyte Interfaces*, 182nd ECS Meeting; Electrochemical Society: Toronto, 1992.

(31) (a) Bain, C. D.; Whitesides, G. M. *J. Am. Chem. Soc.* **1989**, *111*, 7164. (b) Rowe, G. K.; Creager, S. E. *Langmuir* **1994**, *10*, 1186.

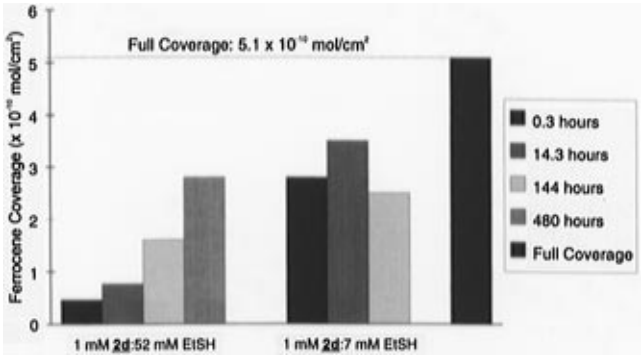

Figure 6. Chart depicting **2d** coadsorption with ethanethiol. Electrochemically assessed coverage is plotted as a function of soaking time.

0.68×10^{-10} mol/cm^2, respectively. Assuming complete accessibility of the ferrocenyl groups, this reflects a 27% accessibility of the azobenzene redox centers. Repeated cycling to -2.3 V (vs Fc/Fc$^+$) results in desorption of **2d**, as evidenced by a decrease in the waves associated with the azobenzene and ferrocenyl groups. However, the ferrocenyl waves decrease in size more rapidly than the azobenzene waves. After 10 cycles the electrochemical accessibilities of the ferrocenyl and azobenzene groups are 1.2×10^{-10} and 0.38×10^{-10} mol/cm^2, respectively (Figure 5B). This reflects a 32% accessibility of the azobenzene redox centers. Apparently as the molecules are desorbed from the surface, free volume is introduced into the film, which results in increased, but not complete, azobenzene electrochemical accessibility.

Also, it is worth noting that the surface ratio of **2d** to ethanethiol was significantly affected by soaking time and the solution ratio of **2d** to ethanethiol. Au(111)/mica was soaked in 1:7 and 1:50 mM ratios of **2d** to ethanethiol in cyclohexane over lengths of time from 20 min to 20 days. Over time the electrochemical accessibility, and, presumably the surface coverage, of **2d** continues to increase until it reaches a limiting value of $\sim 3 \times 10^{-10}$ mol/cm^2, Figure 6. This characteristic of longer chain thiols slowly approaching a limiting submonolayer coverage value has been observed by Bain and Whitesides for coadsorbed alcohol and methyl-terminated alkanethiols on Au[31a] and by Rowe and Creager for ferrocenylhexanethiols and alkanethiols on Au.[31b] By contrast they observed that coadsorbed methyl-terminated alkanethiols on Au apparently reached their final surface equilibria overnight. Chidsey et. al. observed that coadsorbed ferrocenyl- and methyl-terminated alkanethiols also reached their final surface concentrations quickly.[29] Our results suggest a much slower dynamic process with this set of adsorbate molecules and that the monolayer formation process is very molecule and condition dependent.

The small redox waves associated with the reduction of azobenzene groups in a monolayer film of **2d** in aprotic media also may be explained by the dense packing of the monolayer. Several studies have examined the electrochemical responses of redox-active species trapped within a SAM.[28b,31b,32] In contrast to redox-active species at the periphery of the film, moieties trapped within the film exhibit broadened waves at potentials further removed from the potentials which effect those processes when the redox groups are freely accessible to charge-compensating ions. A voltammetry simulation program provided by Creager based on a double-layer model developed by White[30,32,33] estimated the reduction potential of **2d** to be -17.4 V vs Fc/Fc$^+$ if the anion charge is localized near the N═N bond. In a molecular system, the localization of the radical electron near the N═N bond in azobenzene compounds has been verified by EPR.[34] While this exceedingly large number is most likely due in part to limitations in the double-layer model such as effects of electrolyte anions, functional groups, and solvent,[32] this large negative potential shift does imply that azobenzene reduction in SAMs of **2d** is unlikely in our electrochemical potential window. The reason for this large potential shift is that charge-compensating cations are physically separated from the azobenzene groups in the densely packed film. The small azobenzene waves that are observed in the voltammograms are believed to be due to minority azobenzene sites (N═N groups) in the film that are accessible to charge-compensating *n*-Bu$_4$N$^+$ cations. The number of "defect sites" and naturally available free volume in the film dictate the magnitude of these waves. In protic media, where the hydrazobenzene is formed upon reduction of the film, structural changes associated with the conversion of the planar azobenzene moiety[35] to the kinked hydrazobenzene compound[36] must also decrease the magnitude of azobenzene electrochemical accessibility.

It should be noted that the incorporation of the ferrocenyl group into these azobenzene-based monolayers not only serves as an internal reference but also enhances the charge-blocking effects of these films, presumably by further burying the azobenzene groups in the hydrophobic film. For example, the azobenzene groups in SAMs of **1d** on Au are slightly electrochemically accessible, as evidenced by the small reversible redox wave at -1.96 V vs Fc/Fc$^+$ in Figure 3A. A similar wave is not observed in the cyclic voltammetry of **2d** under comparable conditions, Figure 3B.

Ion-Gated Electron Transfer Self-Assembled Monolayers of 2d. The effect that we are reporting herein is proposed, in part, to be a consequence of physically separating the charge-compensating cations from the sites of reduction in the film. If our hypothesis is correct, it should be possible to "gate" or trigger the electron transfer processes between the Au electrode and the buried azobenzene groups by adjusting the size and concentration of the charge-compensating cations. Figure 7A shows the cyclic voltammogram of a film of **2d** on Au(111) after an adsorption time of 1 h in THF/0.1 M *n*-Bu$_4$NPF$_6$. The voltammogram exhibits almost no azobenzene electrochemical accessibility ($\sim$2%). By adding H$_2$O or LiBF$_4$, the system is offered a smaller charge-compensating cation (H$^+$ or Li$^+$) and the electrochemical accessibility of the azobenzene groups is substantially increased. Figure 7B shows the cyclic voltammogram of a film of **2d** on Au(111) prepared in this fashion with 1 M H$_2$O added. Approximately 40% of the azobenzene groups within the film of **2d** on Au are electrochemically reduced to the hydrazobenzene species when H$_2$O is present. A similar effect is observed with the use of LiBF$_4$ accessibility (see the supporting information). The short soaking time is used to prepare a more loosely packed film ($\sim$50% of a full monolayer) with greater potential for ion gating. Films formed from longer soaking times (full monolayers) exhibit similar responses but with lower azobenzene accessibility ($\sim$20% for Li$^+$ and $\sim$30% for H$^+$).

(32) (a) Rowe, G. K.; Creager, S. E. *J. Phys. Chem.* **1994**, *98*, 5500. (b) Rowe, G. K.; Creager, S. E. *Langmuir* **1991**, *7*, 2307.

(33) Model conditions: 1.04 nm from the azobenzene redox center to the film/solution interface; 1.06 nm from the azobenzene redox center to the film/electrode interface; film dielectric constant, 2.56; THF dielectric constant, 7.32; electrolyte concentration, 100 mol/m^3; surface concentration of the redox species, 5.1×10^{-6} mol/m^2; $E_{1/2}$ of one-electron azobenzene reduction in solution, -1.91 V vs Fc/Fc$^+$; potential of zero charge for the electrode, -0.58 V vs Fc/Fc$^+$; temperature, 298 K; scan rate, 0.2 V/s.

(34) (a) Strom, E. T.; Russell, G. A.; Konaka, R. *J. Chem. Phys.* **1965**, 42, 2033. (b) Johnson, C. S., Jr.; Chang, R. *J. Chem. Phys.* **1965**, 43, 3183.

(35) Bouwstra, J. A.; Schouten, A.; Kroon, J. *Acta. Crystallogr. C* **1983**, 39, 1121.

(36) Pestena, D. C.; Power, P. P. *Inorg. Chem.* **1991**, 30, 528.

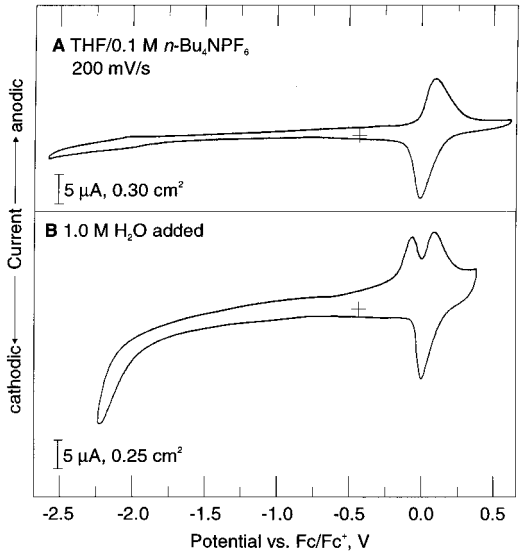

Figure 7. Ion-gating: (A) Cyclic voltammetry for a film of **2d** on Au(111)/mica (soaking time 1 h) in THF/0.1 M *n*-Bu_4NPF_6 electrolyte (large cation source). (B) Cyclic voltammetry for a film of **2d** on Au-(111)/mica (soaking time 1 h) in THF/0.1 M *n*-Bu_4NPF_6 electrolyte and 1 M H_2O (small cation source).

Finally, the electrochemistry for SAMs of **1d** and **2d** on Au was examined as a function of H^+ concentration in aqueous Britton−Robinson buffers over the pH range 3−12. The monolayers are stable to repeated cycling in the pH range from 4 to 11. Unfortunately, for SAMs of **2d** on Au, the reduction of ferrocenylazobenzene has a large pH dependence and E_{pc} moves outside of the solvent potential window below pH 7. However, for SAMs of **1d** on Au, the monolayers exhibit a pH dependence such that $E_{1/2} = 0.50\ V \times pH - 0.36\ V$ (vs SCE) in the pH range from 4 to 11.

Summary of Electrochemical Measurements. Azobenzene-terminated adsorbate molecules in SAMs pack tightly enough to severely inhibit ion penetration. Therefore, in conventional solvents/electrolytes, the electrochemical accessibilities of the azobenzene groups in SAMs formed from **1d** and **2d** are inhibited because the films physically prohibit charge-compensating cations from entering them. By this model, the only azobenzene reduction that does occur is at locations of free volume in the SAM where the cations can penetrate the film. Addition of free volume to the film by coadsorption of diluents with **1d** or **2d** or more efficient use of the existing free volume with smaller cations results in greater azobenzene accessibility. Addition of the ferrocenyl group to **1d** (to form **2d**) decreases the azobenzene accessibility whereas the ferrocenyl group at the film surface is completely electrochemically accessible.

The azobenzene SAMs therefore bear resemblances to many biological membrane systems in their ability to discriminate between cations of differing sizes. In membrane systems, groups of molecules self-assemble to create channels or gates through which only specific ion types can pass.[15] SAMs of **1d** and **2d** also exhibit size selectivity and allow small ions to enter the films but prohibit large ions from doing so. SAMs of **2d** are particularly efficient at regulating ion transport to the redox-active azobenzene centers. Incorporation of free volume into the films, by either coadsorption methods (*vide supra*) or using a different substrate,[4a,37] which by virtue of its surface coordination chemistry spaces out adsorbate molecules in a monolayer film, is analogous to increasing the pore channel diameter in biological systems. In both cases the penetrability of large cations is substantially increased.

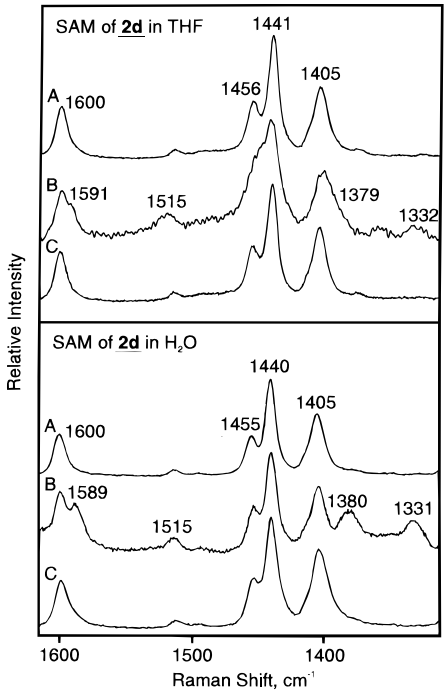

Figure 8. Top spectral series: Raman spectroelectrochemical studies of **2d** on Au in THF/0.1 M *n*-Bu_4NPF_6 electrolyte at (A) 0 V vs Ag/AgCl, (B) −1.7 V vs Ag/AgCl, and (C) back at 0 V vs Ag/AgCl (λ_{ex} = 752 nm, 15 mW, collection time 30 s). Bottom spectral series: Raman spectroelectrochemical studies of **2d** on Au in H_2O/0.2 M $NaClO_4$ electrolyte at (A) 0 V vs Ag/AgCl, (B) −0.7 V vs Ag/AgCl, and (C) back at 0 V vs Ag/AgCl (λ_{ex} = 633 nm, 10 mW, collection time 30 s).

Infrared External Reflection Spectroscopy and Surface-Enhanced Raman (SER) Spectroelectrochemistry. Infrared external reflection spectroscopy was performed on SAMs of **1d** and **2d** on large Au(111)/mica substrates. Weak adsorbate-based bands were observed at 1256 cm^{-1} for SAMs of **1d** and at 1600 and 1265 cm^{-1} for SAMs of **2d**. However, the weakness of the infrared signals motivated us to concentrate our efforts on Raman spectral analysis, where we can take advantage of SERS.

The results of Raman spectroelectrochemical studies of SAMs of **2d** in THF/0.1 M *n*-Bu_4NPF_6 (Figure 8, top series) and in $H_2O/NaClO_4$ (Figure 8, bottom series) verify the formation of the hydrazobenzene product in both media when the electrode is held at a potential sufficiently negative to reduce solution **2d**. In both cases, spectrum A is of the SAM of **2d** before azobenzene reduction is effected, and spectrum C is of the SAM after the holding experiment is complete and the working electrode potential has returned to zero. Note that the bands at 1600, 1456, 1440, and 1405 cm^{-1} are representative of SAMs of **2d**, and that the process, therefore, is chemically reversible.[14a] For both media, spectrum B shows loss in signal intensity for these bands and concomitant growth of bands at 1589, 1515, 1380, and 1331 cm^{-1}. Since in H_2O and other protic media the reduction product of azobenzene is hydrazobenzene, we assign the new bands in the THF experiment, which are comparable to those observed in H_2O, to surface-confined ferrocenylhydrazobenzene. The relative intensities of the bands associated with the hydrazobenzene in the two experiments (in H_2O and in THF) must be interpreted carefully since the two experiments were performed with different excitation wavelengths. The experiment in H_2O involved a 633 nm excitation source while the experiment in THF employed a 752 nm

(37) Chen, K.; Herr, B. R.; Singewald, E. T.; Mirkin, C. A. *Langmuir* **1992**, 8, 2585.

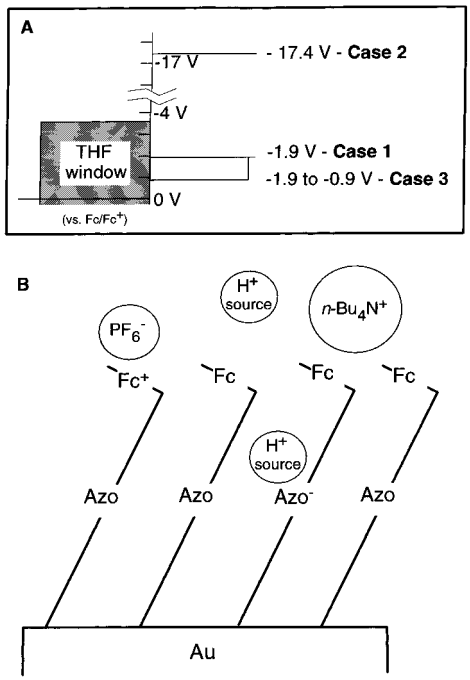

Figure 9. (A) Energy diagram depicting the azobenzene reduction processes discussed in this paper. Note: Case 2 also comprises a range of potentials that depend on the relative positions and environments for the azobenzene groups within the film. One potential is given for one set of conditions; see ref 33. (B) Scheme depicting the selective penetration of small cations and proton sources into a SAM of **2d**.

excitation source. Because the former, but not the latter, excitation wavelength overlaps both the solution and solid-state UV−vis spectra of **2d**, the spectrum taken in H_2O is additionally enhanced by electronic resonance effects.[14a] The fact that the hydrazobenzene is formed in THF under these conditions illustrates how sensitive the azobenzene films are to protons and how difficult it is to eliminate proton effects from electrochemical measurements of these azobenzene SAMs.[4a,b] Note that the results of these spectroelectrochemical experiments mirror our observations involving the cyclic voltammetry of SAMs of **2d**.

The SERS spectra of surface-confined **2d** also change reversibly upon oxidation of the ferrocenyl groups. The pair of bands at 1456 and 1440 cm^{-1} collapse into a single band at 1456 cm^{-1}. A similar spectral difference was observed between **2d** in THF solution and its analogue oxidized by $AgPF_6$ in THF solution. This spectroscopically verifies complete accessibility of the ferrocenyl group in this novel redox bilayer as hypothesized earlier on the basis of cyclic voltammetry experiments involving SAMs of **2d**.

Conclusions. We have detailed the preparation and characterization of SAMs formed from surface-confinable azobenzene- and ferrocenylazobenzene-terminated butanethiols on Au. Adsorption of these molecules onto Au surfaces has been verified by X-ray photoelectron spectroscopy and reflectance infrared spectroscopy. Optical ellipsometry, capacitance measurements, and cyclic voltammetry indicate that these adsorbate molecules form densely packed, highly oriented monolayer films on Au. The electrochemical azobenzene reduction processes for surface-confined **2d** are summarized by the energy diagram in Figure 9A. Case 1 represents reduction of azobenzene groups to the radical anion species when these groups are accessible to aprotic charge-compensating cations (n-Bu_4N^+) in THF/0.1 M n-Bu_4NPF_6 (at minority sites at full monolayer coverage); this process occurs at a potential (−1.9 V vs Fc/Fc^+) comparable to that necessary for effecting reduction of solution **2d**. Case 2 reflects the reduction potentials for azobenzenes that are buried in densely packed SAMs of **2d** (and even **1d**), which resist the incorporation of charge-compensating cations. When the azobenzene redox sites within a SAM are inaccessible toward cations, their reduction potentials are reductively shifted outside the potential window of the electrochemical experiments, represented by case 2. Therefore, in a SAM of **2d** at full monolayer coverage in THF/0.1 M n-Bu_4NPF_6, only relatively few azobenzene groups near sites of free volume are accessible electrochemically (case 1). Addition of free volume to the film by coadsorption with ethanethiol or more efficient use of the existing free volume with smaller cations such as H^+ or Li^+ results in greater azobenzene accessibility. Reduction of the azobenzene groups in the SAM in the presence of H^+ results in hydrazobenzene formation, which has been verified by SER spectroelectrochemistry. The reduction potential of the azobenzene group varies with proton concentration (−1.9 to −0.9 V vs Fc/Fc^+), and is represented by case 3. The selective penetration of small cations (or proton sources) into a SAM of **2d** is depicted in Figure 9B. Addition of the ferrocenyl group to the azobenzene group slightly reduces the azobenzene accessibility whereas the ferrocenyl layer at the film/solution interface is completely electrochemically accessible.

It is worth noting that the property of SAMs referred to as charge blocking (e.g., Figure 4A,C) is not the same as the property referred to as ion-gating herein. The former property is associated with a film's (or any material's) ability to passivate the electrode surface over large areas. In the case of a monolayer, the passivation property is independent of molecular orientation. The ion-gating behavior that we are reporting in this paper is not only dependent on dense packing but also highly dependent on the orientation of the azobenzene groups with respect to the electrode surface and the solution/film interface. If the azobenzene groups were oriented in parallel fashion with the electrode surface and resided at the solution/film interface, they would exhibit normal electrochemical behavior. Furthermore, charge blocking depends more on macroscopic uniformity of the film while ion-gating is highly dependent on the microscopic film structure and uniformity. Indeed, a Au electrode that is partially bare and partially modified with a densely packed monolayer of **2d** does not exhibit charge blocking of ferricyanide ions but does exhibit ion-gating (see the supporting information).

It is interesting that the ferrocenyl groups in SAMs of **2d** are electrochemically active even though the ferricyanide ions are electrochemically inactive when probed with an electrode modified with a SAM of **2d.** Two factors can account for this disparity. First, the ferrocenyl oxidation can be catalyzed by a small number of sites that are more accessible to the electrode surface. This argument has been used to explain the electrochemical accessibility of redox groups in other SAM-based systems.[1d,28b] Second, covalent attachment of redox groups to the azobenzene alkane tether is likely to increase the rate of electron transfer as compared with noncovalently bound redox groups for statistical (the covalently bound group is always held at the film/solution interface) and electronic reasons. The first factor is dominant in monolayers that are formed from the pure redox-active adsorbate molecule, and the second becomes increasingly important in mixed monolayers formed from redox-active and redox-inactive adsorbate molecules. Also, the hydrophobic ferrocenyl group is likely to partition into the monolayer much better than the hydrophilic ferricyanide ions, which would be expected to increase the electrochemical accessibility and rate of electron transfer for the ferrocenyl group as compared with ferricyanide ion.

In conclusion, the redox activity of the surface-confined azobenzene moiety has been shown to be highly dependent upon monolayer structure. Significantly, the novel ferrocenylazobenzene SAM structure allows one to gate electron transfer processes between the electrode surface and redox sites buried several angstroms within a monolayer by controlling the size and concentration of charge-compensating cations in solution. This gating behavior constitutes a supramolecular response in SAMs as it is a collective property of the film and not a property of the molecules that comprise the film.

This paper underscores the importance of understanding the relationship between monolayer structure and electron transfer processes. In general, understanding the factors that control SAM formation for adsorbate molecules which contain electrochemically, photochemically, and chemically reactive functionalities ultimately will provide greater predictability of the chemical and physical properties of materials constructed from SAM methodology.

Acknowledgment. C.A.M. acknowledges the Office of Naval Research (Grant URI3136YIP) for support of this work. C.A.M. also acknowledges a NSF NYI Award (Grant CHE-9121859), a Camille Dreyfus Teacher-Scholar Award, an A. P. Sloan Foundation Fellowship, and a DuPont Young Professor Award. C.A.M. also acknowledges support by the MRSEC Program of the National Science Foundation, at the Materials Research Center of Northwestern University, under Award No. DMR-9120521. R.P.V.D. acknowledges support by the National Science Foundation (Grant CHE-940078). B.R.H. acknowledges a Henkel Corporation Research Fellowship in Colloid and Surface Chemistry. Professors Henry White and Stephen Creager are gratefully acknowledged for helpful discussion and comments. In addition, we thank S. Creager for the computer simulation program used to model the electrochemical processes for the SAM of **2d**.

Supporting Information Available: Expanded experimental and synthetic details for **1a**−**d** and **2a**−**d**, Li^+-gated electron transfer behavior for an SAM of **2d**, and details of the experiment differentiating charge-blocking and ion-gating behavior of SAMs of **2d** (11 pages). See any current masthead page for ordering and Internet access instructions.

JA961873P